The inhibitory effect of EGCG-AgNP-lysozyme bioconjugates on biofilm formation

Brahmaiah Meesaragandla,[1,2] Shahar Hayet,[3,4] Tamir Fine,[3,4] Una Janke[1,2,] Liraz Chai,[3,4] and Mihaela Delcea[1,2,5]**

[1]Institute of Biochemistry, University of Greifswald, Felix-Hausdorff-Straße 4, 17489 Greifswald, Germany

[2]ZIK HIKE - Zentrum für Innovationskompetenz „Humorale Immunreaktionen bei kardiovaskulären Erkrankungen“, Fleischmannstraße 42, 17489 Greifswald, Germany

[3]Institute of Chemistry, The Hebrew University of Jerusalem, Edmond J. Safra Campus, Jerusalem 91904, Israel

[4]The Center for Nanoscience and Nanotechnology, The Hebrew University of Jerusalem, Edmond J. Safra Campus, Jerusalem 91904, Israel

[5]DZHK (Deutsches Zentrum für Herz-Kreislauf-Forschung), partner site Greifswald, Germany

KEYWORDS. AgNPs, EGCG, human lysozyme, conformational change, antibacterial activity

ABSTRACT

Multidrug resistance of pathogenic bacteria to antimicrobial drugs has become a major problem for the diagnosis and treatment of infectious diseases. Here, we report on the synthesis of silver nanoparticles (AgNPs) with epigallocatechin gallate (EGCG) ligand, which is known to present antibacterial activity. We further describe the interaction of EGCG-AgNPs with lysozyme, an antibacterial enzyme abundant in fluids like serum, saliva and tears, and the formation of EGCG-AgNP-lysozyme bioconjugates. Our results demonstrate the formation of lysozyme protein corona as shown by UV-Vis, dynamic light scattering and SDS-PAGE analyses. Using circular dichroism spectroscopy we found that lysozyme preserves its secondary structure at low concentration of EGCG-AgNPs, whereas higher concentrations induce protein structural changes. Furthermore, we have shown in bacterial growth and biofilm formation assays that EGCG presents no antibacterial activity on planktonic Bacillus subtilis cells when it was bound to AgNPs. It was found that EGCG-AgNPs (>40 nM) inhibit B. subtilis in biofilm forming conditions and the inhibition effect is reduced by lysozyme corona formation on EGCG-AgNPs. Our results demonstrate that EGCG-AgNPs could be used as antibiofilm agents because they showed lower cytotoxicity and significant inhibitory effect on pellicle formation.

Introduction

Multidrug resistance of pathogenic bacteria to antimicrobial drugs has become a major concern toward successful diagnosis and treatment of various pathogenic diseases.[1] Recently, development of nanotechnology-based antimicrobial agents has gained importance for fighting multidrug resistance in microorganisms. One of such materials are silver nanoparticles (AgNPs) which exhibit a broad spectrum of antibacterial and antifungal properties.[2-5] The antibacterial activity of AgNPs involves several mechanisms; for example, AgNPs can release Ag^+ ions and can produce radical species after penetration of AgNPs inside the cells/bacteria leading to deregulation of important cellular mechanisms and cellular damage and death.[6] Moreover, AgNPs are one of the most predominant nanomaterials in various products i.e fabrics, bandages, deodorizers, food containers and disinfectants.[7-15] This is due to their excellent optoelectronic properties i.e surface plasmon resonance, and small size, high surface-to-volume ratio and their cost effectiveness. Also, nanosilver is comparatively less reactive than silver ions and is suitable for clinical and therapeutic applications.[16-17] AgNPs exhibit different degrees of antimicrobial activity depending on their shape, size and surface chemistry. In addition, coating the AgNPs with cationic ligands and other antimicrobial molecules can further improve their antimicrobial activity due to synergistic effects.[18]

(-)-Epigallocatechin gallate (EGCG) is one of the dominant catechins present in green tea and exhibits various therapeutic properties including anti-obesity, anti-inflammatory, antidiabetic, antitumor effects and antibacterial activity.[19-22] Additionally, EGCG is a strong antioxidant, which has been reported to exhibit anti-cancer activity against various cancers (e.g., brain, prostate, pancreatic, and bladder) by inducing apoptosis.[23-30] Li et al. have shown that EGCG can change protein surface polarity and reversibly inhibit β-ketoasil (asil transport protein) reductase

(FabG) reversibility from bacteria. As a result, the modified enzyme (EGCG-FabG complex) undergoes aggregation, and can kill the bacterial cells.[31] On oral administration of EGCG, the rate of ingestion is less than 5% in humans and below 1% in rats.[32-34] Such low EGCG bioavailability confines its bioactivity in vivo. One way to improve the adsorption of EGCG is to adsorb EGCG molecules on AgNPs, which provide large adsorbent surface per unit mass due to their small size.

Nanoparticles, as drug delivery agents, can be administered in many ways, including oral, nasal, intraocular and parenteral. After coming in contact with biological media, nanoparticles can interact with proteins forming a so-called protein corona and may alter protein structure and its activity. Among all proteins, lysozyme is an antibacterial enzyme which catalyzes the hydrolysis of β1,4-glucosidic linkages between N-acetylglucosamine (NAG) and N-acetylmuramic acid (NAM) in peptidoglycan of the cell wall, particularly in Gram-positive bacteria.[35] Lysozyme is a small, monomeric, and globular protein, abundant in various body fluids including serum (4-13 mg/L), saliva, tears and human milk.[36-38] It consists of 130 amino acid residues with a molecular mass of 14.3 kDa and belongs to the α+β class of proteins. The compact structure of lysozyme is stabilized by four disulfide bonds and its surface is typically polar, whereas its inner part is almost hydrophobic. It is an alkaline molecule (isoelectric point = 11.35) and positively charged in aqueous solutions. It has been shown that antibacterial activity of lysozyme is more susceptible for Gram-positive bacteria than for Gram-negative bacteria.[39-40] However, lysozyme simply loses its antibacterial activity when exposed to blood or environment. The antibacterial activity of lysozyme can be enhanced when its antibacterial spectrum is broadened by adding other bactericides.[41] Therefore, the study of the interaction of EGCG-AgNPs with lysozyme is necessary to evaluate the antimicrobial activity of EGCG-AgNP-lysozyme conjugates.

In the present study, we have synthesized EGCG-AgNPs and investigated their interaction with human lysozyme at physiological temperature. We have studied the antibacterial activity of EGCG-AgNPs and their lysozyme bioconjugates (EGCG-Ag-lysozyme) against the Gram-positive wild type bacterium Bacillus subtilis through bacterial growth and biofilm formation assays. Biofilms are colonies of bacteria held together by an extracellular matrix which provides mechanical stability and increases antibiotic resistance.[42-43] In addition, cytotoxicity assays of EGCG-AgNPs and their conjugates with lysozyme on the human umbilical vein endothelial cells were carried out. This study helps to design EGCG-AgNPs as effective and safe antimicrobial agents.

Results and Discussion

Synthesis and characterization of EGCG-AgNPs.

AgNPs were prepared by the reduction of $AgNO_3$ in the presence of EGCG, a polyphenol used as reducing agent as well as stabilizing agent due to the availability of hydroxyl (-OH) groups. The formation of AgNPs was confirmed by the occurrence of surface plasmon resonance (SPR) band in the UV-Vis spectrum which displayed a characteristic absorption band at 413 nm (Figure 1A). TEM analysis showed spherical EGCG-AuNPs with sizes of 14 ± 4.5 nm (Figure 1B), whereas DLS showed an hydrodynamic diameter (d_H) of 36 ± 2.39 nm and 126 ± 10.39 nm (Figure 1C). The increase in the d_H around 36 nm compared to ~ 14 nm in the TEM results might be explained by the formation of a EGCG-AgNPs dimer, whereas the d_H around 126 nm might be due to the formation of some aggregated complexes of EGCG-AgNPs in water. Figure S1A and S1B show the time-dependent UV-Vis spectra of EGCG-AgNPs in water and PBS (pH 6.2), respectively. No significant changes in the absorption band position and intensity were observed over time, indicating that the synthesized EGCG-AgNPs are quite stable in water (Figure S1A).

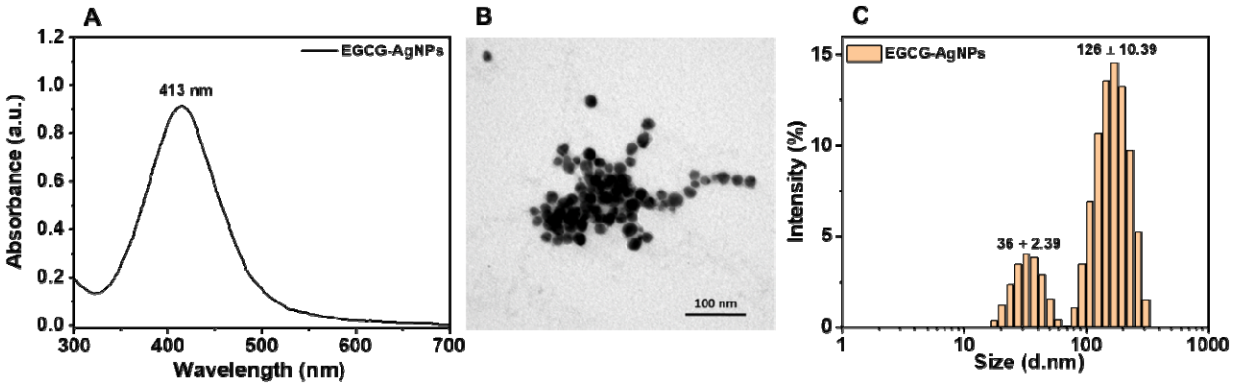

Figure 1. UV-Visible spectrum (A), TEM image (B) and size distribution (C) of EGCG-AgNPs in water.

In contrast, we have observed a blue shift of SPR band from 413 nm to 401 nm for the EGCG-AgNPs as soon as they were added into PBS buffer (Figure S1B). Furthermore, the intensity of the SPR band decreased with time indicating the instability of AgNPs in PBS buffer. Our data suggest that EGCG-AgNPs are stable in water due to -OH and -OH interactions between EGCG molecules and unstable in PBS due to the disruption of these interactions on the NPs surface leading to change in the refractive index on the AgNPs surface. This was further supported by increased negative zeta potential values of EGCG-AgNPs in PBS (-35 mV) when compared to water (-27 mV) (Figure S2).

Interactions of human lysozyme with EGCG-AgNPs

The interaction of lysozyme with EGCG-AgNPs in PBS (pH 6.2) was characterized by UV-Vis, DLS and zeta potential analyses. Firstly, we fixed the concentration of lysozyme (6.8 µM) and added different concentrations of EGCG-AgNPs and incubated for 3 h at 37 □. A red shift in the absorption band from 413 nm to 424 nm was observed for the EGCG-AgNPs as soon as they were added in PBS buffer containing lysozyme (Figure 2A). Interestingly, no change in the intensity and SPR band position was observed even after incubation at 37 □ for 3 h (Figure 2B). The shift in the absorption band towards longer wavelength without change in the intensity

suggests strong interactions between EGCG-AgNPs and lysozyme molecules. This was also supported by an increase in the overall d_H for EGCG-AgNP-lysozyme bioconjugates (Figure 2C).

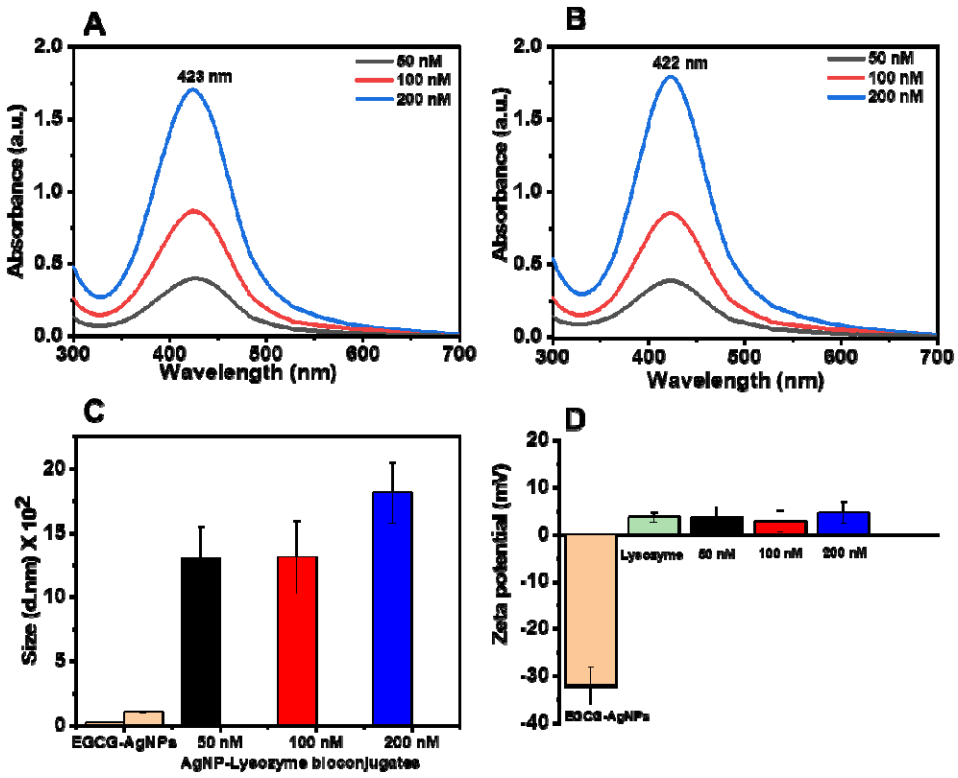

Figure 2. UV-Visible spectra of EGCG-AgNP-lysozyme bioconjugates before (A) and after 3 h (B) incubation in PBS buffer (pH 6.2) at 37 □. d_H of EGCG-AgNPs and their AgNP-lysozyme bioconjugates after 3 h incubation (C). ζ-Potential of EGCG-AgNPs, lysozyme, and their corresponding AgNP-lysozyme bioconjugates at pH 6.2 (D). Lysozyme concentration was fixed to 6.8 µM and AgNPs concentration was varied (50, 100, 200 nM).

However, the increase in the d_H for AgNP-lysozyme bioconjugates without affecting the SPR peak position and intensity suggests that the increase in size is not due to AgNP aggregation. The EGCG-AgNP-lysozyme interaction might be due to strong binding between EGCG molecules and lysozyme molecules. The increase of the AgNPs d_H in the presence of lysozyme is accompanied by a decrease in the zeta potential (Figure 2D). EGCG-AgNPs showed a positive

surface charge after conjugation with lysozyme, indicating that lysozyme adsorbed onto the EGCG-AgNPs, forming EGCG-AgNP-lysozyme bioconjugates.

Secondly, we have increased the lysozyme concentration (6.8, 20.4, 34 μM) and fixed the EGCG-AgNPs concentration (100 nM) to monitor shifts in the absorption peak of EGCG-AgNPs (Figure S3). However, we did not observe any shift in the absorption peak, irrespective of EGCG-AgNPs and lysozyme concentrations. This indicates that EGCG-AgNPs can form stable EGCG-AgNP-lysozyme bioconjugates with lysozyme, irrespective of either EGCG-AgNPs or lysozyme protein concentrations.

Furthermore, the presence of lysozyme on EGCG-AgNPs was assessed by SDS-PAGE. Figure S4 depicts the SDS-PAGE gel revealing the protein adsorption to the differently concentrated EGCG-AgNPs. The first lane shows the protein marker with a band around 14 kDa for the lysozyme. As expected, EGCG-AgNPs showed no protein bands, while strong protein bands were observable for the bioconjugates similar to free lysozyme as control.

Effect of EGCG-AgNPs on the secondary structure of lysozyme.

Figure 3 shows the CD spectra of lysozyme alone and lysozyme with EGCG-AgNPs in varying concentrations. The CD spectra of lysozyme exhibit two negative minima at 208 nm and 222 nm, suggesting a significant α-helical content. These two peaks are contributed by the $\pi-\pi^*$ and $n-\pi^*$ transitions of the peptide bonds, respectively.[44]

The ellipticity values of lysozyme at both peak wavelengths become more negative after 3 h incubation at 37 °C, indicating an increase in the α-helical content of lysozyme at physiological temperature. Interestingly, the intensity and shape of CD spectra were found to be dependent on the concentration of EGCG-AgNPs. For example, increased ellipticity values were observed for

the lysozyme after immediate addition of low concentration of EGCG-AgNPs (10 nM), Figure 3A, but the shape and intensity of ellipticity values remained unchanged even after 3 h incubation with 10 nM EGCG-AgNPs (Figure 3B). However, decreased ellipticity values were observed with increasing the concentration of EGCG-AgNPs; almost change to β-sheet structure at higher concentrations of EGCG-AgNPs (100 nM, 200 nM). This suggests that the structure of lysozyme is stable and showed the regular α-helix rich conformation at lower concentration of EGCG-AgNPs (10 nM), whereas turns to β-sheet rich conformation at higher concentrations of EGCG-AgNPs (100 nM / 200nM).

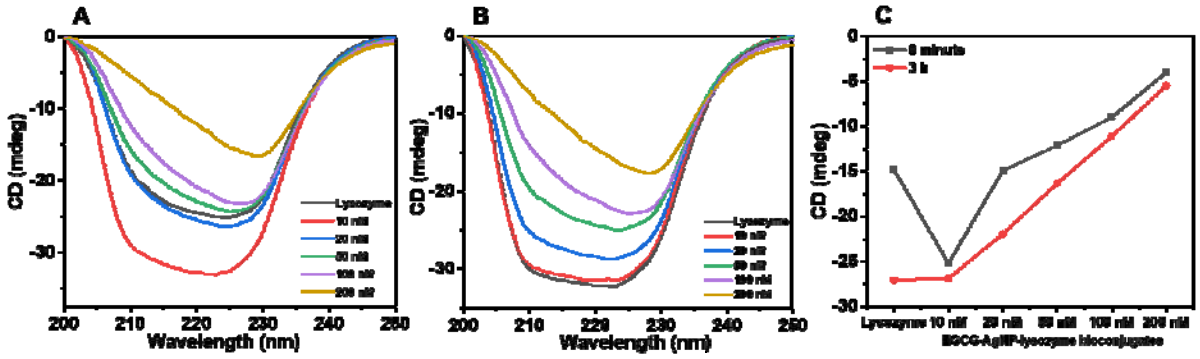

Figure 3. CD spectra of human lysozyme (6.8 µM) in free from and in EGCG-Ag-lysozyme bioconjugates with increased concentrations of AgNPs in PBS buffer (pH 6.2) before (A) and after 3 h (B) incubation at 37 □. (C) Plot of ellipticity values at 208 nm for lysozyme and AgNP-lysozyme bioconjugates at pH 6.2.

We believe that the structural changes of lysozyme with the EGCG-AgNPs might be due to the strong hydrogen bonding interaction between the EGCG and lysozyme molecules. α-helical and β-sheet structures of the lysozyme are mostly stabilized by hydrogen bonds, which results in rigid protein structure. Instead, hydrogen bonding does not exist in β-turn and random coil structure, which lead to more flexibility in protein structure. EGCG has many -OH groups which may interact with lysozyme molecules *via* hydrogen bonding and make them more stable at low

concentration of EGCG-AgNPs. With increasing EGCG-AgNPs concentrations, inter-hydrogen bonding interactions between the EGCG and lysozyme molecules become more dominant which may unfold the structure of lysozyme resulting in β-sheet rich conformation. The fractional contents of the secondary structures calculated by the Bestsel software are presented in Table S1. As shown in Table S1, a reduction in the α-helical fraction of the lysozyme from 20.5% to 3.4 % was observed in the presence of EGCG-AgNPs (200 nM) after 3 h incubation. The CD spectroscopy analyses show that the interaction of EGCG-AgNPs with human lysozyme causes fewer changes in the secondary structure of the protein, this is an increase in the α-helical contents at low concentration of EGCG-AgNPs at room temperature and decrease in the α-helical contents with increased concentrations of NPs at physiological temperature; indicating that lysozyme preserves its secondary structure at low NP concentration and undergoes structural changes at higher NP concentration.

Effect of EGCG-AgNPs and EGCG-AgNP-lysozyme bioconjugates on *Bacillus subtilis* bacterial growth and in biofilm forming conditions

We examined the effect of the EGCG-AgNPs and EGCG-AgNP-lysozyme bioconjugates on cell viability and biofilm formation of WT *B. subtilis*. Surprisingly, despite the antibacterial activity of free EGCG on *B. subtilis* cells,[45] EGCG showed no antibacterial activity on planktonic *B. subtilis* cells when it was bound to AgNPs, as indicated by the similarity of the *B. subtilis* growth curves in the presence and in the absence of EGCG-AgNPs (Figure 4A). However, EGCG-AgNPs at concentrations larger than 40 nM inhibited *B. subtilis* in biofilm forming conditions. Inhibition of biofilm formation in EGCG-AgNP concentrations that are not biocidal to the cells suggests that the EGCG-AgNPs affect biofilm formation pathways rather than through cellular proliferation processes.

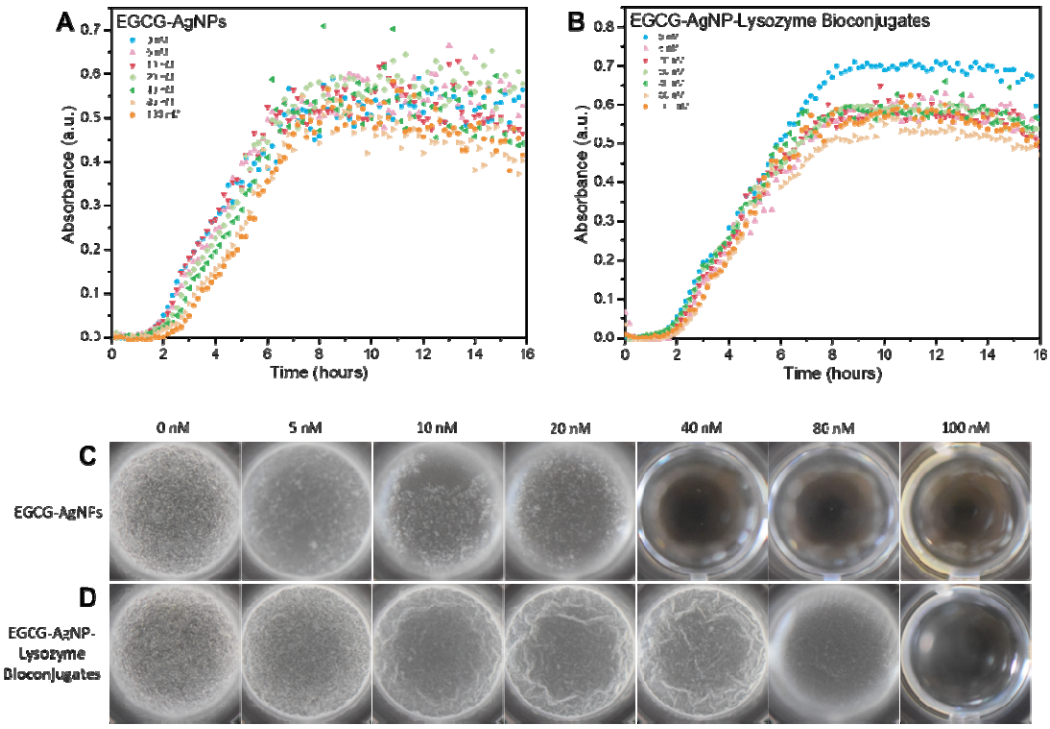

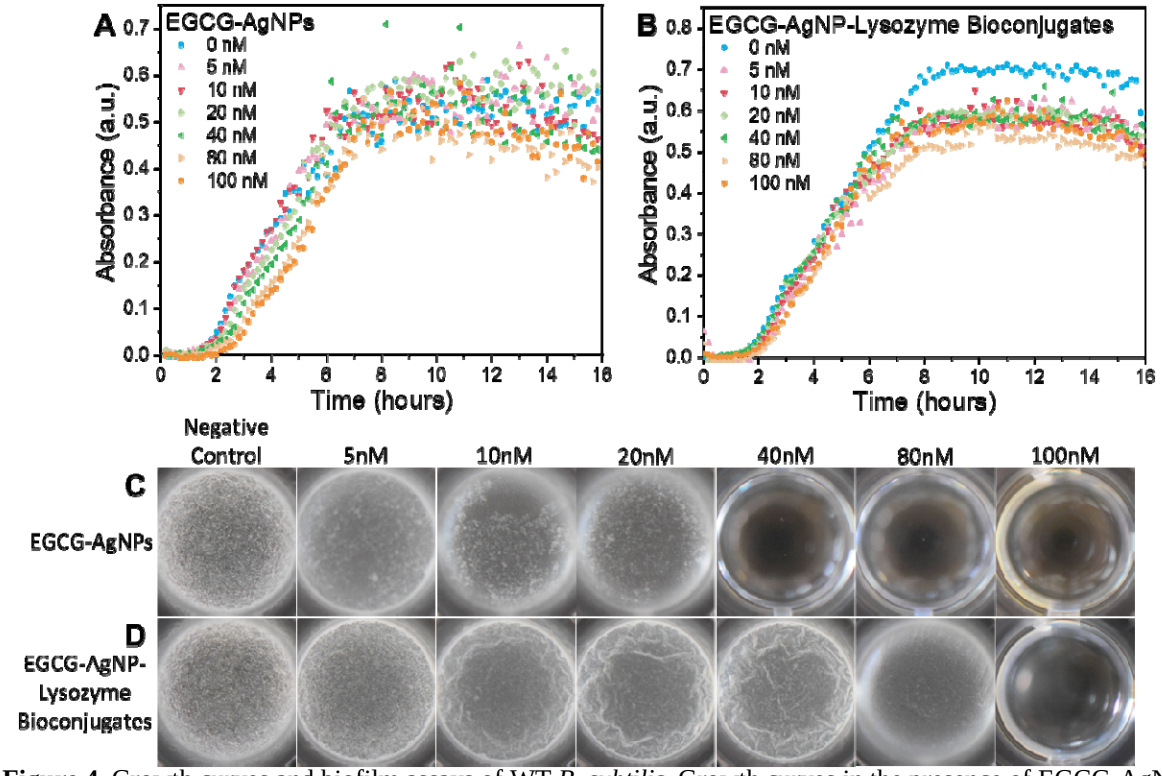

Figure 4. Growth curves and biofilm assays of WT *B. subtilis*. Growth curves in the presence of EGCG-AgNPs (A)

and in the presence of EGCG-AgNP-lysozyme bioconjugates in PBS at pH 6.2 (B). The concentration of the NPs is specified in the legends. Biofilm formation by *B. subtilis* in the absence and in the presence of increasing concentrations of EGCG-AgNPs (C) and EGCG-AgNP-lysozyme bioconjugates (D).

Similarly to EGCG-AgNPs, when these NPs were additionally functionalized with lysozyme, they showed no biocidal activity on *B. subtilis* cells in the concentration range we have used. However, the lysozyme corona reduced the effect of EGCG-AgNPs on *B. subtilis* biofilms. Specifically, biofilm inhibition occurred at concentrations larger than 80 nM EGCG-AgNPs-lysozyme bioconjugates, which is larger than the 40 nM cutoff concentration for biofilm inhibition by EGCG-AgNPs. It has been proposed that the bactericidal action of EGCG is due to the negatively charged EGCG moieties combined with the positively-charged bacterial lipid polysaccharide membrane and can generate hydrogen peroxide (H_2O_2), which damages the bacterial membrane.[46-47] The decrease in the inhibition of biofilm by the EGCG-AgNPs-lysozyme bioconjugates might be either due to the blockage of negatively charged EGCG moieties by the lysozyme or lysozyme may lose its lytic activity against bacterial cell wall when it is bound to EGCG-AgNPs.

In order to investigate any salt influence on the inhibitory effect of EGCG-AgNPs-lysozyme bioconjugates, we slightly decreased the sodium ion concentration in PBS and studied their inhibitory effect on *B. subtillis*. Interestingly, EGCG-AgNPs-lysozyme bioconjugates showed an improvement in the inhibitory effect, whereas no change was observed for EGCG-AgNPs. In particular, the inhibitory concentration of the EGCG-AgNPs-lysozyme bioconjugates was reduced from 80 nM (at high salt concentration) to 40 nM, which is similar to EGCG-AgNPs without lysozyme, (Figure S5B). Removal of salt additionally leads to cell growth curve

inhibition, which was not observed in PBS (Figure S5A). We believe that a strong inhibition of EGCG-AgNPs-lysozyme bioconjugates at a reduced salt concentration might be due to the alteration of lysozyme conformation and exposure of negatively charged EGCG moieties that are otherwise buried; changes of the conformation of lysozyme may therefore reactivate the activity of EGCG, and lead to similar activity to that of EGCG-AgNPs that do not have a lysozyme corona.

Cytotoxicity of EGCG-AgNPs and EGCG-AgNPs-lysozyme bioconjugates

We have investigated the toxicity of EGCG-AgNPs and EGCG-AgNPs-lysozyme bioconjugates on HUVEC cells as model system for endothelial cells, which are forming the inner layer of blood vessels. Figure 5 shows the cell viability data after treatment with different concentrations of EGCG-AgNPs, EGCG-AgNP-lysozyme bioconjugates for HUVEC cells. EGCG-AgNPs present a lower cytotoxicity when compared to EGCG-AgNPs-lysozyme bioconjugates. However, with increasing concentration of EGCG-AgNPs, a decrease in cell viability was observed. A very strong toxicity was seen at a concentration of 100 nM AgNPs. EGCG-Ag-lysozyme bioconjugates showed decreased cell viability compared to EGCG-AgNPs even at lower concentrations. This might be due to either formation of aggregated complexes or faster uptake rates by cells of the lysozyme bioconjugates.

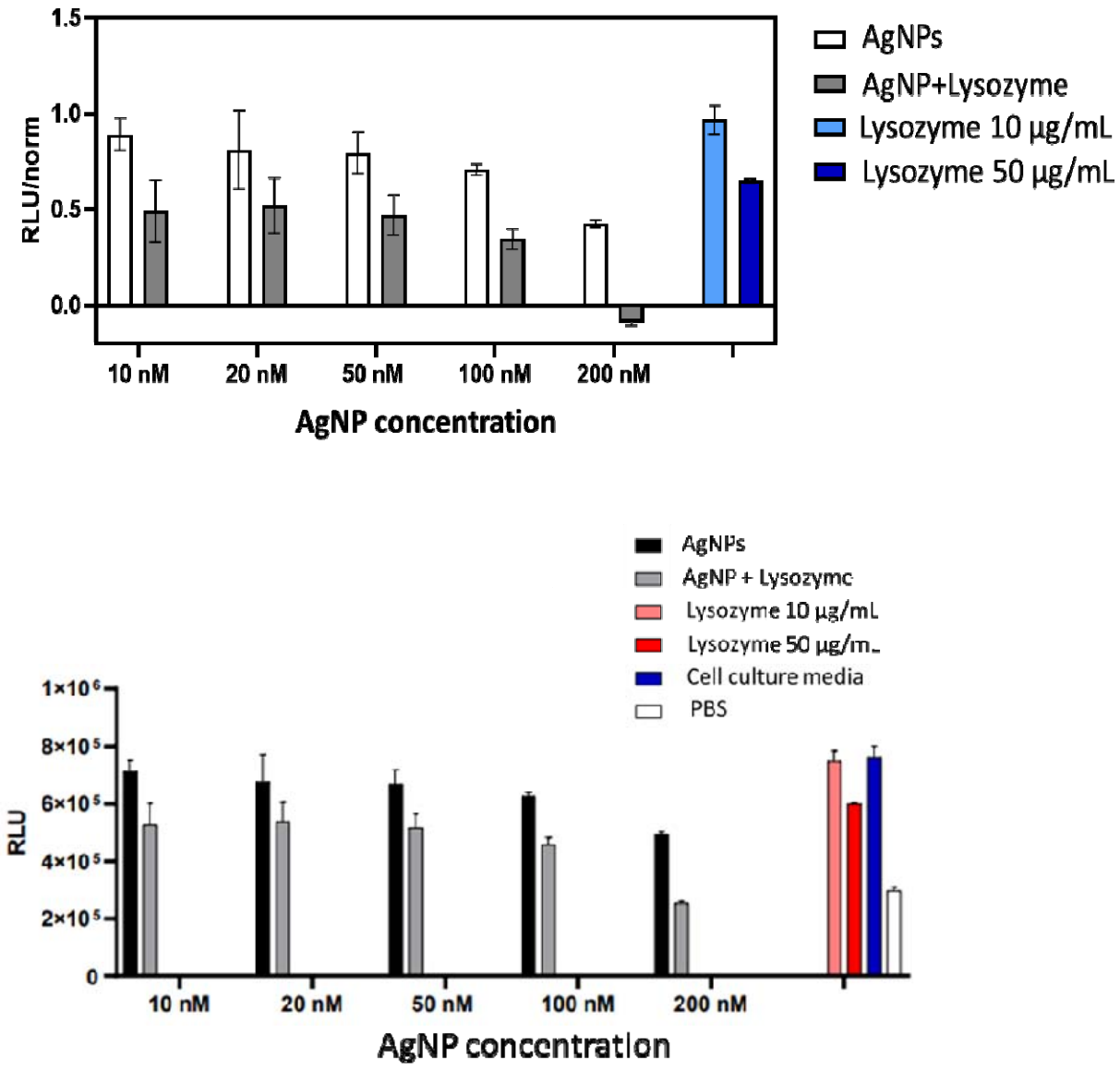

Figure 5. Cytotoxicity assay of HUVEC cells for different concentrated EGCG-AgNPs (10, 20, 50, 100, 200 nM) and the corresponding AgNP-lysozyme bioconjugates in endothelial cell culture media supplemented with fetal bovine serum (FBS). Measurement data was normalized as explained in the method section.

Conclusions:

We have studied the interaction of EGCG-AgNPs with human antibacterial enzyme lysozyme and their inhibitory effect on Gram-positive wild type *B. subtlilis* bacteria. By CD spectroscopy we found that changes in the secondary structure of the lysozyme protein depend on the

concentration of AgNPs. EGCG-AgNPs and their lysozyme bioconjugates exhibited a strong inhibition of *B. subtlilis* biofilm formation at 40 nM and 80 nM, respectively. We have shown that a reduction in the salt concentration can increase the inhibitory activity of lysozyme bioconjugates. Our results demonstrate that EGCG-AgNPs could be used as a antibiofilm agent against *B. subtlilis* as they showed lower toxicity and significant inhibitory effect on pellicle formation.

Experimental section:

Materials. Human lysozyme, phosphate buffer saline (PBS) and silver nitrate ($AgNO_3$) were purchased from Sigma-Aldrich (Taufkirchen, Germany). EtOH, HCl, and NaOH were purchased from Roth (Karlsruhe, Germany). The concentration of lysozyme was measured spectrophotometrically using a molar extinction coefficient of 5734 $mol^{-1}cm^{-1}$ at 280 nm. The water used was purified through an ultrapure water system, Millipore system Sartorius Stedim Biotech (Göttingen, Germany).

20 mM sodium phosphate buffer was prepared from sodium phosphate monobasic and dibasic. PBS was prepared by dissolving 0.137 M NaCl, 0.0027 M KCl, 0.01 M Na_2HPO_4, 0.0018 M KH_2PO_4 in triple-distilled water (TDW) and adjusting for pH with HCl. Except NaCl, all chemicals were purchased from Sigma-Aldrich (Darmstadt, Germany). NaCl was purchased from J.T. Baker-Avantor (Center Valley, PA, USA). The water was purified through Barnstead GenPure water purification system (Thermo Scientific).

Epigallocatechin gallate (EGCG)-AgNPs. 9.99 mM EGCG solution was prepared by dissolving 4.58 mg of EGCG in 1 mL deionized water which was pre-adjusted with pH 8, and then it was added dropwise in 30 ml of 1mM $AgNO_3$ (5.03 mg in 30 mL water) solution with

continuous stirring at 27 □ for 2 h. $AgNO_3$ solution turned from colourless to violet upon addition of EGCG solution.

EGCG-AgNPs-Lysozyme interaction. EGCG-AgNPs were added to the lysozyme containing PBS (pH 6.2) and the mixture was incubated at 37 □ for 3 h prior to characterization. For the analysis of protein structural changes, a fixed concentration of lysozyme (100 μg mL^{-1}) was mixed with various concentrations of EGCG-AgNPs (10, 20, 50, 100, 200 nM) and then incubated at 37 □ for 3 h. Similarly, various concentrations of lysozyme (100, 300 and 500 μg/mL) were used for UV-Vis analyses.

EGCG-AgNPs-lysozyme bioconjugates. EGCG-AgNPs (1μM stock solution) were added in PBS buffer (pH 6.2) containing 100 μg/mL lysozyme and incubated at 37 °C for 4 h. EGCG-AgNP-lysozyme bioconjugates were obtained by centrifuging the above mixture at 17,000 g at room temperature for 30 min and resuspending in PBS buffer. The bioconjugates were diluted with PBS buffer to various concentrations (5, 10, 20, 50, 80, 100 nM).

Circular dichroism spectroscopy measurements. The far-UV circular dichroism (CD) spectra of lysozyme before and after incubation with AgNPs were recorded on chirascan spectrophotometer (Applied Photophysics, Leatherhead, UK). The spectrophotometer was purged with nitrogen gas before starting the experiments. Measurements were scanned between 200 and 250 nm with an average of 5 scans using a 5 mm path length cuvette (Hellma Analytics, Müllheim, Germany). All spectra were measured at room temperature with a band width of 1.0 nm. The final data was obtained by subtracting the buffer contribution from the original protein spectra. The fractional contents of the secondary structures were calculated by the Bestsel software.[48]

UV-Vis absorption spectroscopy. DeNovix DS-11 FX+ spectrophotometer (Biozym Scientific GmbH, Germany) was used to obtain the absorption spectra for EGCG-AgNPs, and the same after interacting with lysozyme. All the samples were measured between 200 to 850 nm using 10 mm path length cuvette at room temperature.

Dynamic light scattering (DLS) and zeta potential measurements. Hydrodynamic diameter (d_H) and zeta potential for EGCG-AgNPs and the corresponding lysozyme bioconjugates were determined using Zetasizer Ultra (Malvern Instruments, Kassel, Germany). Except lysozyme bioconjugates, all the samples were prepared as described above and filtered through a 0.2 µm filter. Before measurements, samples were equilibrated for 10 min at room temperature. Each size measurement was recorded allowing 20 runs per measurement with a run duration of 5 s. The average of five separate measurements were used to assess the d_H of the samples. DTS1070 cells were used to measure the zeta potential of AgNPs and their lysozyme bioconjugates. A voltage of 180/40 V was used for the samples measured in deionized distilled water and PBS, respectively. All measurements were acquired at room temperature with an equilibration time of 5 min (20 runs per each measurement) between each measurement. The reported zeta potential is an average of five independent measurements.

Transmission Electron Microscopy. The flotation method was used for the negative staining procedure. AgNPs were allowed to adsorb onto a glow-discharged Pioloform carbon-coated 400-mesh grid for 5 min. The grid was then transferred onto two droplets of deionized water and finally onto a drop of 1 % aqueous uranyl acetate for 30 s. After blotting with filter paper and air-drying, the samples were examined with a transmission electron microscope LEO 906 (Carl Zeiss Microscopy Deutschland GmbH, Oberkochen, Germany) at an acceleration voltage of 80 kV. For image acquisition, a wide-angle dual speed CCD camera Sharpeye (Tröndle,

Moorenweis, Germany) was used, operated by the ImageSP software. All micrographs were edited by using Adobe Photoshop CS6.

SDS-PAGE. SDS-PAGE was carried out to detect lysozyme in EGCG-AgNP-lysozyme bioconjugates under reductive conditions. Therefore, EGCG-AgNP-lysozyme bioconjugates and EGCG-AgNPs were centrifuged twice at 20,000 g at RT for 40 min and resuspended in 50 µl PBS buffer. All samples were denatured for 5 min in reducing SDS sample buffer at 95 °C and loaded to 12 % Tris-Gylcine SDS gel together with a Novex™ Sharp Unstained Protein Standard (Invitrogen, Carlsbad, USA). The gel was visualized with the Pierce Silver Stain Kit (Thermo Fischer, Darmstadt, Germany).

Biofilm and Growth Curve Assays. Liquid culture of WT *B. subtilis* was grown in LB broth at 37 °C for 16 h. For biofilm formation assays, 2 µL of starting culture were added to 88 µL of MSgg medium in a 96-well plate and incubated (24 h, 30 °C) with 10 µL EGCG-AGNPs or with EGCG-AgNP-lysozyme bioconjugates to achieve various final concentrations: 5, 10, 20, 40, 80, and 100 nM. Biofilms were captured with a Nikon D3300 camera with a micro Nikkor 85mm lense. For growth curve assay, 2 µL of starting culture were added to 88 µL of LB broth in a 96-well plate with 10 µL EGCG-AgNP-Lysozyme bioconjugates in various final concentrations, as specified above for biofilms. Bacterial growth was measured in a microplate reader (Tecan Spark 10M, Tecan Trading AG, Switzerland) for 16 h at 37 °C with 180 RPM orbital shaking. Assays were repeated similarly with 20 mM sodium phosphate buffer pH 6.2.

EGCG-AgNPs stock solutions were prepared in TDW, and EGCG-AgNPs-lysozyme stock solutions were prepared in PBS buffer. Control experiments without EGCG-AgNPs were

performed with water as a substitute of EGCG-AgNPs and PBS buffer as substitute for EGCG-AgNP-lysozyme bioconjugates.

Cell Viability Assay. Cell viability assays were carried out following manufacturer's instructions from the CellTiter-Glo 2.0 assay from Promega (Madison, USA). In brief, 5×10^4 human umbilical vein endothelial cells (HUVEC)/mL were seeded in endothelial cell growth medium MV (Promocell, Heidelberg, Germany) with SupplementMix. Cells were incubated for 3 h in an opaque 96-well plate at 37 °C and 5% CO_2. Then, media was removed and different concentrations of AgNPs were added, indicated in the respective graphs. After 24 h incubation at 37 °C and 5% CO_2, 100 µl of CellTiter-Glo 2.0 was added to each well and luminescence signal was measured in a Cytation 5 imaging reader (BioTek instruments Inc., Winooske, USA) after 10 min incubation.

ASSOCIATED CONTENT

Supporting Information.

UV-Vis absorption spectra and Zeta potential of EGCG-AgNPs in water and PBS; UV-Visible spectra of EGCG-AgNP-lysozyme bioconjugates; SDS-PAGE analysis for EGCG-AgNP-lysozyme conjugates; Percentages of secondary structures of lysozyme in presence of EGCG-AgNPs at pH 6.2; Growth curves and pellicle assays of wild type *B. subtilis* in the presence of EGCG-AgNP-lysozyme bioconjugates in 20 mM sodium phosphate buffer at pH 6.2.

AUTHOR INFORMATION

Corresponding Author

Liraz Chai: liraz.chai@mail.huji.ac.il

Mihaela Delcea: delceam@uni-greifswald.de

ACKNOWLEDGMENT

We acknowledge Dr. Rabea Schlüter (University of Greifswald) for TEM analyses. BM and MD acknowledge the German Federal Ministry of Education and Research (BMBF) for the financial support (project NanoImmun FKZ03Z22C51).

REFERENCES

1. Desselberger, U. Emerging and re-emerging infectious diseases. *J. Infect.* **2000**, *40*, 3-15.
2. Morones, J. R.; Elechiguerra, J. L.; Camacho, A.; Holt, K.; Kouri, J. B.; Ramírez, J. T.; et al. The bactericidal effect of silver nanoparticles. *Nanotechnology* **2005**, *16*, 2346-2353.
3. Kim, J. S.; Kuk, E.; Yu, K. N.; Kim, J. H.; Park, S. J.; Lee, H. J.; et al. Antimicrobial effects of silver nanoparticles. *Nanomed. Nanotechnol. Biol. Med.* **2007**, *3*, 95-101.
4. Panácek, A.; Kolár, M.; Vecerová, R.; Prucek, R.; Soukupová, J.; Krystof, V.; et al. Antifungal activity of silver nanoparticles against Candida spp. *Biomaterials* **2009**, *30*, 6333-6340.
5. Namasivayam, S. K. R.; Ganesh, S.; Avimanyu, B. Evaluation of antibacterial activity of silver nanoparticles synthesized from Candida glabrata and Fusarium oxysporum. *Int. J. Med. Res.* **2011**, *1*, 131-136.
6. Talapko, J.; Matijevi´c, T.; Juzbaši´c, M.; Antolovi´c-Požgain, A.; Škrlec, I. Antibacterial Activity of Silver and Its Application in Dentistry, Cardiology and Dermatology. *Microorganisms* **2020**, *8*, 1400.
7. Benn, T. M.; Westerhoff, P. Nanoparticle silver released into water from commercially available sock fabrics. *Environ Sci Technol* **2008**, *42*, 4133-4139.
8. Sönnichsen, C.; Reinhard, B. M.; Liphardt, J.; Alivisatos, A.P. A molecular ruler based on plasmon coupling of single gold and silver nanoparticles. *Nat. Biotechnol.* **2005**, *23*, 741-745. 9. Vanamudan, A.; Sudhakar, P.P. Biopolymer capped silver nanoparticles with potential for multifaceted applications. *Int. J. Biol. Macromolec.* **2016**, *86*, 262-268.
10. Salata O. V. Applications of nanoparticles in biology and medicine. *J Nanobiotechnol.* **2004**, 2, 1-6.
11. Panacek A.; Kvítek, L.; Prucek, R.; Kolár, M.; Vecerova R.; Pizúrova, N. et al. Silver colloid nanoparticles: synthesis, characterization, and their antibacterial activity. *J Phys Chem*. **2006**, *110*, 16248-53.
12. Yoshida, K.; Tanagawa, M.; Atsuta, M. Characterization and inhibitory effect of antibacterial dental resin composites incorporating silver-supported materials. *J. Biomed Mater Res* **1999**, *47*, 516-522.
13. Ider, M.; Abderrafi, K.; Eddahbi, A.; Ouaskit, S.; Kassiba, A. Rapid synthesis of silver nanoparticles by microwave-polyol method with the assistance of latex copolymer. *J. Cluster Sci*. **2017**, *28*, 1025-1040.
14. Shim, I. K.; Lee, Y.; Lee, K.J.; Joung, J. An organometallic route to highly monodispersed silver nanoparticles and their application to ink-jet printing. *Mater. Chem. Phys.* **2008**, *110*, 316-321.
15. Davenas, J.; Ltaief, A.; Barlier, V.; Boiteux, G.; Bouazizi, A. Nanomaterials for photovoltaic conversion. *Mater. Sci. Eng. C* **2008**, *28*, 744-750.
16. Kim, J. Y.; Sungeun, K.; Kim, J.; Jongchan, L.; Yoon, J. The biocidal activity of nano-sized silver particles comparing with silver ion. *Korean Soc. Environ. Eng.* **2005**, *27*, 771-776.
17. Chen, X.; Schluesener, H. J. Nanosilver: a nanoproduct in medical application. *Toxicol. Appl. Pharmacol. Lett.* **2008**, *176*, 1-12.
18. Ashraf, S.; Akhtar, N.; Ghauri, M. A.; Rajoka, M. I.; Khalid, Z. M.; Hussain, I. Polyhexamethylene biguanide functionalized cationic silver nanoparticles for enhanced antimicrobial activity. *Nanoscale Res Lett.* **2012**, *7*, 267-273.
19. Balentine, D. A.; Wiseman, S. A.; Bouwens, L. C. M. The chemistry of tea flavonoids. *Crit. Rev. Food Sci. Nutr.* **1997**, *37*, 693-704.
20. Du, G.-J.; Zhang, Z.; Wen, X.-D.; Yu, C.; Calway, T.; Yuan, C.-S.; Wang, C.-Z. Epigallocatechin Gallate (EGCG) Is the Most Effective Cancer Chemopreventive Polyphenol in Green Tea. *Nutrients* **2012**, *4*, 1679-1691.
21. Haque, S. A.; Cañete, S. J. P. HPLC-CUPRAC post-column derivatization method for the determination of antioxidants: A performance comparison between porous silica and core-shell column packing. *J. Anal. Sci. Technol.* **2018**, *9*, 4.

22. Radhakrishnan, R.; Kulhari, H.; Pooja, D.; Gudem, S.; Bhargava, S.; Shukla, R.; Sistla, R. Encapsulation of biophenolic phytochemical EGCG within lipid nanoparticles enhances its stability and cytotoxicity against cancer. *Chem. Phys. Lipids.* **2016**, *198*, 51-60.
23. Jung, Y. D.; Kim, M. S.; Chay, K. O.; Ahn, B. W.; Liu, W.; Bucana, C. D.; Gallick, G. E.; Ellis, L. M. Jung, Y., Kim, M., Shin, B. et al. EGCG, a major component of green tea, inhibits tumour growth by inhibiting VEGF induction in human colon carcinoma cells. *Br. J. Cancer* **2001**, *84*, 844-850.
24. Annabi, B.; Bouzeghrane, M.; Moumdjian, R.; Moghrabi, A.; Beliveau, R. Probing the infiltrating character of brain tumors: inhibition of RhoA/ROK-mediated CD44 cell surface shedding from glioma cells by the green tea catechin EGCg. *J. Neurochem.* **2005**, *94*, 906-916. 25. Chung, L. Y.; Cheung, T. C.; Kong, S. K.; Fung, K. P.; Choy, Y. M.; Chan, Z. Y.; Kwok, T. T. Induction of apoptosis by green tea catechins in human prostate cancer DU145 cells. *Life Sci.* **2001**, *68*, 1207-1214.
26. Ahn, W. S.; Huh, S. W.; Bae, S.-M.; Lee, I. P.; Lee, J. M.; Namkoong, S. E.; Kim, C. K.; Sin, J.-I. A major constituent of green tea, EGCG, inhibits the growth of a human cervical cancer cell line, CaSki cells, through apoptosis, G(1) arrest, and regulation of gene expression. *DNA Cell Biol.* **2003**, *22*, 217-224.
27. Kemberling, J. K.; Hampton, J. A.; Keck, R. W.; Gomez, M. A.; Selman, S. H. Inhibition of Bladder Tumor Growth by the Green Tea Derivative Epigallocatechin-3-Gallate. *J. Urol.* **2003**, *170*, 773-776.
28. Valcic, S.; Timmermann, B. N.; Alberts, D. S.; Wächter, G. A.; Krutzsch, M.; Wymer, J.; Guillén, J. M. Inhibitory effect of six green tea catechins and caffeine on the growth of four selected human tumor cell lines. *Anticancer Drugs* **1996**, *7*, 461-468.
29. Gensler, H. L.; Timmermann, B. N.; Valcic, S.; Wächter, G. A.; Dorr, R.; Dvorakova, K.; Alberts, D. S. Prevention of photocarcinogenesis by topical administration of pure epigallocatechin gallate isolated from green tea. *Nutr. Cancer.* **1996**, *26*, 325-335.
30. Barthelman, M.; Bair III, W. B.; Stickland, K. K.; Chen, W.; Timmermann, B. N.; Valcic, S.; Dong, Z.; Bowden, G. T. (-)-Epigallocatechin-3-gallate inhibition of ultraviolet B-induced AP-1 activity. *Carcinogenesis* **1998**, *19*, 2201-2204.
31. Li, B.H.; Zhang, R.; Du, Y.T.; Sun, Y.H.; Tian, W.X. Inactivation mechanism of the β-ketoacyl-[acyl carrier protein] reductase of bacterial type-II fatty acid synthase by epigallocatechin gallate. *Biochem. Cell Biol.* **2006**, *84*, 755-762.
32. Nagle, D. G.; Ferreira, D.; Zhou, Y.-D. Epigallocatechin-3-gallate (EGCG): chemical and biomedical perspectives. *Phytochemistry* **2006**, *67*, 1849-1855.
33. Zhu, M.; Chen, Y.; Li, R. C. Oral Absorption and Bioavailability of Tea Catechins. *Planta Med.* **2000**, *66*, 444-447.
34. Yang, C. S.; Chen, L.; Lee, M. J.; Balentine, D.; Kuo, M. C.; Schantz, S. P. Blood and urine levels of tea catechins after ingestion of different amounts of green tea by human volunteers. *Cancer Epidemiol. Biomarkers Prev.* **1998**, *7*, 351-354.
35. Cegielska-Radziejewska, R.; Lesnierowski, G.; Kijowski, J. Antibacterial activity of hen egg white lysozyme modified by thermochemical technique. *Eur. Food Res. Technol.* **2009**, 228, 841-845.
36. Ren, D.; Yi, H.; Wang, W.; Ma, X. The enzymatic degradation and swelling properties of chitosan matrices with different degrees of N-acetylation. *Carbohydrate Research* **2005**, *340*, 2403-2410.
37. Yoshimura, K.; Toibana, A.; Nakahama, K. Human lysozyme: sequencing of a cDNA, and expression and secretion by Saccharomyces cerevisiae. *Biochem. Biophys. Res. Commun*. **1988**, *150*, 794-801.
38. Pepys, M. B.; Hawkins, P. N.; Booth, D. R.; Vigushin, D. M.; Tennent, G. A.; Soutar, A. K. et al. Human lysozyme gene mutations cause hereditary systemic amyloidosis. *Nature* **1993**, 362, 553-557.
39. Wu, T.; Wu, C.; Fu, S.; Wang, L.; Yuan, C.; Chen, S.; Hu, Y. Integration of lysozyme into chitosan nanoparticles for improving antibacterial activity. *Carbohydrate Polymers* **2017**, *155*, 192-200.

40. Yuan, S.; Yin, J.; Jiang, W.; Liang, B.; Pehkonen, S.O.; C. Enhancing antibacterial activity of surface-grafted chitosan with immobilized lysozyme on bioinspired stainless steel substrates. *Colloids and Surfaces B: Biointerfaces* **2013**, *106*, 11-21.

41. Chen, X.; Niyonsaba, F. H.; Okuda, D.; Nagaoka, I.; Ikeda, S.; Okumura, K., et al. Synergistic effect of antibacterial agents human beta-defensins, cathelicidin ll-37 and lysozyme against Staphylococcus aureus and Escherichia coli. *Journal of Dermatological Science* **2005**, *40*, 123-132.
42. Flemming, H. C.; Wingender, J.; Szewzyk, U. *et al*. Biofilms: an emergent form of bacterial life. *Nat Rev Microbiol* **2016**, *14***,** 563–575.

43. Costerton, J. W.; Lewandowski, Z.; Caldwell, D. E.; Korber, D. R.; Lappin-Scott, H. M. *Annual Review of Microbiology* **1995** 49:1, 711-745.

44. Besley, N. A.; Hirst, J. D. Theoretical Studies toward Quantitative Protein Circular Dichroism Calculations. *J. Am. Chem. Soc.* **1999**, *121*, 9636-9644.

45. Nakayama, M.; Shimatani, K.; Ozawa, T.; Shigemune, N.; Tomiyama, D.; Yui, K.; Katsuki, M.; Ikeda, K.; Nonaka, A.; Miyamoto, T. Mechanism for the antibacterial action of epigallocatechin gallate (EGCg) on Bacillus subtilis, *Bioscience, Biotechnology, and Biochemistry* **2015**, *79*, 845-854.

46. Balentine, D. A.; Wiseman, S. A.; Bouwens, L. C. The chemistry of tea flavonoids. *Crit Rev Food Sci Nutr* **1997**, *37*, 693-704.

47. Arakawa, H.; Maeda, M.; Okubo, S.; Shimamura T. Role of hydrogen peroxide in bactericidal action of catechin. *Biol Pharm Bull* **2004**, *27*, 277-281.

48. Micsonai, A.; Bulyaki, E.; Kardos, J. BeStSel: From Secondary Structure Analysis to Protein Fold Prediction by Circular Dichroism Spectroscopy. *Structural Genomics*, ***2199***, 175-189.